Luke Bouma, December 18, 2016.

$$Q'_{\star/p} = Q'_0 (P_{\rm tide})^{\alpha} (M)^{\beta} (M')^{\gamma} (P_{\rm spin})^{\delta} \quad (1)$$

$$Q'_{\star/p} = \begin{cases} Q'_{\rm eq} (P_{\rm tide})^{\alpha_{\rm eq}} & \text{if } |P_{\rm tide}| < 2P_{\rm spin} \\ Q'_{\rm inr} (P_{\rm tide})^{\alpha_{\rm inr}} & \text{if } |P_{\rm tide}| \geq 2P_{\rm spin} \end{cases} \quad (2)$$

1 MESA stellar evolution grid

`POET` computes the orbital evolution of a system with a single star and a single planet under the influence of tides. The tidal dissipation rate of both the star and the planet depends on the spin period of the body damping the tidal wave (Eq. 1). To assign a dissipation rate, we thus need a prescription for the angular momentum evolution of both the star and planet.

As the star evolves, its convective envelope loses angular momentum to a wind through magnetic braking (Schatzman 1962). We write this loss rate as Eq. XX. In addition, the star's radiative core and convective envelopes exchange angular momentum (Eq. YY). In Eq. YY τ_c is the coupling timescale at which the core and envelope are driven to solid-body rotation.

To find the time-evolution of the stellar quantities in Eqs. XX and YY, namely $R_\star(t), I_{\rm rad}(t), I_{\rm conv}(t), R_{\rm rad}(t)$, and $M_{\rm rad}(t)$, we compute stellar evolutionary tracks using `MESA` (Paxton et al. 2011, 2013, 2015). We specifically follow the work of '`MESA` Isochrones & Stellar Tracks' (MIST)[1], a project that has built and tested large grids of single-star evolution models across all evolutionary phases, for a wide range of masses and metallicities (Dotter 2016, Choi et al. 2016).

In nearly all cases, we adopt the same physics as Choi et al. 2016, hereafter C+16. We downloaded the `MESA` input files (`inlists`) from the MIST website[2] and, subject to minor modifications, directly used them to compute stellar evolutionary tracks across our desired parameter space. That parameter space is defined as:

$$0.4 \leq M_\star/M_\odot \leq 1.2 \quad (0.1 M_\odot \text{ spaced}) \quad (3)$$

$$-1 \leq [\text{Z/H}] \leq 0.5 \quad (0.25\text{dex spaced}), \quad (4)$$

where the grid resolution is primarily limited by convenience (we will interpolate between these grids to match them with measured masses and metallicities of actual stars). We begin each stellar model in its pre-main sequence[3], follow its evolution through its main sequence, and halt it once its He core-mass reaches $0.1 M_\odot$ (this is often when the star is older than the age of the universe, but it is computationally cheap and convenient in later interpolation).

1.1 Adopted physics

Table 1 of C+16 summarizes the physics behind our stellar evolution models (reproduced for reference as Fig. 1). We replicate these assumptions exactly except for two points, both detailed below: *i)* the solar abundance scale, and *ii)* the specifics of transitions between boundary conditions as a function of stellar mass.

1.1.1 Fine-tuned solar abundance scale

While C+16 use the protosolar abundances recommended by Asplund et al. 2009 ($Z_{\odot,\rm protosolar} = 0.0142$), we find, in agreement with the solar model discussed by C+16 (Sec. 4), that replicating the bulk properties of the Sun at its current age requires adopting fine-tuned protosolar abundances. We insist that our stellar grid reproduce the Sun's radius, luminosity, effective temperature to $\lesssim 1\%$ at an age of 4.57 Gyr. We also insist that our models yield an accurate moment of inertia for the Sun (although this is a model-dependent

[1] Currently hosted at `http://waps.cfa.harvard.edu/MIST/index.html`

[2] `http://waps.cfa.harvard.edu/MIST/data/tarballs_v1.0/MESA_files.tar.gz`, `inlists` retrieved 2016-09-20.

[3] "Uniform composition, $T_c = 5 \times 10^5$ K so no nuclear burning, and uniform contraction for enough luminosity to make it fully convective" (`http://mesa.sourceforge.net/star_job_defaults.html`)

Table 1 Summary of the Adopted Physics.

Ingredient	Adopted Prescriptions and Parameters	Section	Reference
Solar Abundance Scale	$X_\odot = 0.7154$, $Y_\odot = 0.2703$, $Z_\odot = 0.0142$	3.1	Asplund et al. (2009)
Equation of State	OPAL+SCVH+MacDonald+HELM+PC	3.2.1	Rogers & Nayfonov (2002); Saumon et al. (1995); MacDonald & Mullan (2012)
Opacity	OPAL Type I for $\log T \gtrsim 4$; Ferguson for $\log T \lesssim 4$; Type I $\rightarrow$ Type II at the end of H burning	3.2.2	Iglesias & Rogers (1993, 1996); Ferguson et al. (2005)
Reaction Rates	JINA REACLIB	3.2.3	Cyburt et al. (2010)
Boundary Conditions	ATLAS12; $\tau = 100$ tables + photosphere tables + gray atmosphere	3.3	Kurucz (1970), Kurucz (1993)
Diffusion	Track five "classes" of species; MS only	3.4	Thoul et al. (1994); Paquette et al. (1986)
Radiation Turbulence	$D_{\rm RT} = 1$	3.4	Morel & Thevenin (2002)
Rotation	solid-body rotation at ZAMS with $v_{\rm ZAMS}/v_{\rm crit} = \Omega_{\rm ZAMS}/\Omega_{\rm crit} = 0.4$	3.5	Paxton et al. (2013)
Convection: Ledoux + MLT	$\alpha_{\rm MLT} = 1.82$, $\nu = 1/3$, $y = 8$	3.6.1	Henyey et al. (1965)
Overshoot	time-dependent, diffusive, $f_{\rm ov,\ core} = 0.0160$, $f_{\rm ov,\ env} = f_{\rm ov,\ sh} = 0.0174$	3.6.2	Herwig (2000)
Semiconvection	$\alpha_{\rm sc} = 0.1$	3.6.3	Langer et al. (1983)
Thermohaline	$\alpha_{\rm th} = 666$	3.6.3	Ulrich (1972); Kippenhahn et al. (1980)
Rotational Mixing	Include SH, ES, GSF, SSI, and DSI with $f_\mu = 0.05$ and $f_c = 1/30$	3.6.4	Heger et al. (2000)
Magnetic Effects	Not currently implemented	3.6.5	
Mass Loss: Low Mass Stars	$\eta_R = 0.1$ for the RGB $\eta_B = 0.2$ for the AGB	3.7.1	Reimers (1975) Blocker (1995)
Mass Loss: High Mass Stars	$\eta_{\rm Dutch} = 1.0$ a combination of wind prescriptions for hot and cool stars and a separate WR wind prescription	3.7.2	Vink et al. (2000, 2001) Nugis & Lamers (2000) de Jager et al. (1988)
Mass Loss: Rotational	$\xi = 0.43$, boost factor capped at 10^4, $\dot{M}_{\rm max} = 10^{-3}\ M_\odot\ {\rm yr}^{-1}$	3.7.3	Langer (1998)

Figure 1: Table 1 of C+16. (Purely for reference)

quantity, we can compare our MESA profiles with independent models from helioseismology). For our stellar evolutionary tracks, we adopt the protosolar abundances of $Y_{\odot,\rm protosolar} = 0.2612$ and $Z_{\odot,\rm protosolar} = 0.0150$, per Table 2 of C+16.[4]

In the general case, we then specify the metallicity [Z/H] = [Fe/H] of a given star with respect to $Z_{\odot,\rm protosolar} = 0.0150$. For instance, [Z/H] $= -1$ corresponds to a metal mass fraction of 0.00150. Given Z, we find the corresponding hydrogen and helium mass fractions via

$$Y_p = 0.249 \tag{5}$$

$$Y = Y_p + \left(\frac{Y_{\odot,\rm protosolar} - Y_p}{Z_{\odot,\rm protosolar}} \right) Z \tag{6}$$

$$X = 1 - Y - Z, \tag{7}$$

where the primordial helium abundance $Y_p = 0.249$ is adopted from the results of the Planck Collaboration (2015). To find the initial mass fractions of ^{1}H, ^{2}H, ^{3}He, ^{4}He (which MESA takes as input), we use the isotopic ratios given by Asplund et al. 2009, Table 3.

1.1.2 Transitions between boundary conditions

C+16 Sec. 3.3 discusses the various options by which one can constrain the temperature and pressure in the outermost cell of a 1D stellar model. As stated by C+16, the MIST tables (and thus, ours) use a grid of 1D plane-parallel atmosphere models computed using ATLAS12 (Kurucz 1970, 1993). These atmosphere models include molecules that heavily influence the opacities of cool dwarfs such as water vapor and titanium monoxide. With the grid of model atmospheres computed, the standard choice is to set the 'boundary' at $\tau = 2/3$ (the photosphere). However, the atmospheres of cooler dwarfs are influenced by molecules that are not included in MESA's interior model calculations. A better choice for cooler dwarfs is thus to set the boundary condition at a deeper optical depth, *e.g.*, at $\tau = 100$. C+16 do this by using the `photosphere_tables` boundary condition for $0.6 - 10 M_\odot$ and the `tau_100_tables` for $0.1 - 0.3 M_\odot$. In the intermediate $0.3 - 0.6 M_\odot$, C+16 compute stellar models separately using each boundary condition, and then

[4]The tension between the Asplund et al. 2009 abundances and helioseismology results is to date unresolved, see Serenelli 2010 'New results on standard solar models' and Bergemann & Serenelli 2014, 'Solar Abundance Problem'.

interpolate between them following the scheme of Dotter (2016). We do something similar, but simpler: defined on our desired stellar mass range of $0.4 - 1.2 M_\odot$, we say:

$$\texttt{Boundary condition table} = \begin{cases} \texttt{photosphere\_tables} & \text{if } 0.6 \leq M_\star/M_\odot < 1.2 \\ \texttt{tau\_100\_tables} & \text{if } 0.4 \leq M_\star/M_\odot < 0.6. \end{cases} \tag{8}$$

Comparing the low-mass tracks we get when reproducing the MIST models more exactly (Sec. 1.3), the difference between our MESA models, which exclusively use `tau_100_tables`, and those of the MIST grids, which interpolate between `tau_100_tables` and `photosphere_tables`, is small[5].

1.2 Comparison to standard solar models

We show our solar calibration in Fig. 2. 'Predicted' values in this plot are: $R_\odot = 6.957 \times 10^{10}\,\mathrm{cm}$, $L_\odot = 3.928 \times 10^{33}\,\mathrm{erg\,s^{-1}}$, $T_{\mathrm{eff},\odot} = 5772\,\mathrm{K}$, and $I_{\mathrm{tot},\odot} = 7.0799 \times 10^{53}\,\mathrm{g\,cm^2} = 0.0736 M_\odot R_\odot^2$, where $M_\odot = 1.988 \times 10^{33}\,\mathrm{g}$. We find the 'predicted' solar total moment of inertia by numerically integrating the density profile of the standard solar model given by Christensen-Dalsgaard et al. 1996. In Fig. 2, we compute and show $I_{\mathrm{tot},\star}$ only for our MESA grids because those of the MIST project are not published (this was one of the main reasons we opted to make our own stellar evolution grids). The fine-tuned MESA model we use in our grids (solid lines) is 'good enough' for our purposes: at the Sun's age, we are at $\lesssim 1\%$ agreement with predicted values in $R_\star, T_{\mathrm{eff},\star}$, and $I_{\star,\mathrm{tot}}$, and $\sim 2\%$ agreement in $L_\star$. The published 'Sun' from C+16's MIST model is further from the expected values on all counts[6].

As a tedious aside, there is no 'standard' value for the Sun's moment of inertia. The quantity is purely model-determined (a direct measurement would require a known torque showing a measurable effect on the Sun), and in a 1D stellar model is computed as

$$I_{\mathrm{tot},\star} = \frac{8\pi}{3} \int_0^{R_\star} r^4 \rho(r) dr. \tag{9}$$

Thus the density profile completely determines the star's total moment of inertia. Various values for $I_{\mathrm{tot},\star}$ are quoted in the literature without specification of the associated model (e.g., in Allen's Astrophysical Quantities (2000), or in Table 19, Ch1 of Yoder's chapter of Global Earth Physics (1995)). An older 'standard' solar model is Table 28.3 of Schwarzschild (1958). Other values are given by M. Bursa et al., Studia Geophysica et Geodaftica (1996), Iorio, Solar Physics, 1:47, (2012), and Komm et al., Astrophysical J., 586, 650, (2003). As a heavily-cited and somewhat-recent 'standard solar model' (and one that 'worked', compared to the recent ones that use Asplund abundances), from this hodge-podge I selected the model of Christensen-Dalsgaard et al, (1996).

1.3 Replicate the MIST profiles

"But Luke!", you say, "you're basically replicating C+16, and Fig. 2 says you're getting slightly different results! How can we be sure that you know what you're doing?" Answer: by replicating the actual MIST profiles to the best of my ability, following the description from C+16 and their published `inlists`. This gives Fig. 3.

1.4 The actual grid in $M_\star$ and Z

Satisfied with our sanity checks, the resulting grid of stellar evolutionary tracks is attached in TABLE, and with select models shown in Fig. 4.

[5] See the plots in `results/writeup_plots/MESA_MIST_comparison`

[6] N.b. the plotted C+16 MIST model is the actual model used in the main MIST grids, not the 'fine-tuned' solar model discussed in C+16 Sec. 4. The latter might do better than our MESA-computed model, but is not published. We obtain the plotted model by downloading the relevant 'EEP track' from the MIST website, `http://waps.cfa.harvard.edu/MIST/data/tarballs_v1.0/MIST_v1.0_feh_p0.00_afe_p0.0_vvcrit0.4_EEPS.tar.gz`, and taking the `00100M.track.eep` model.

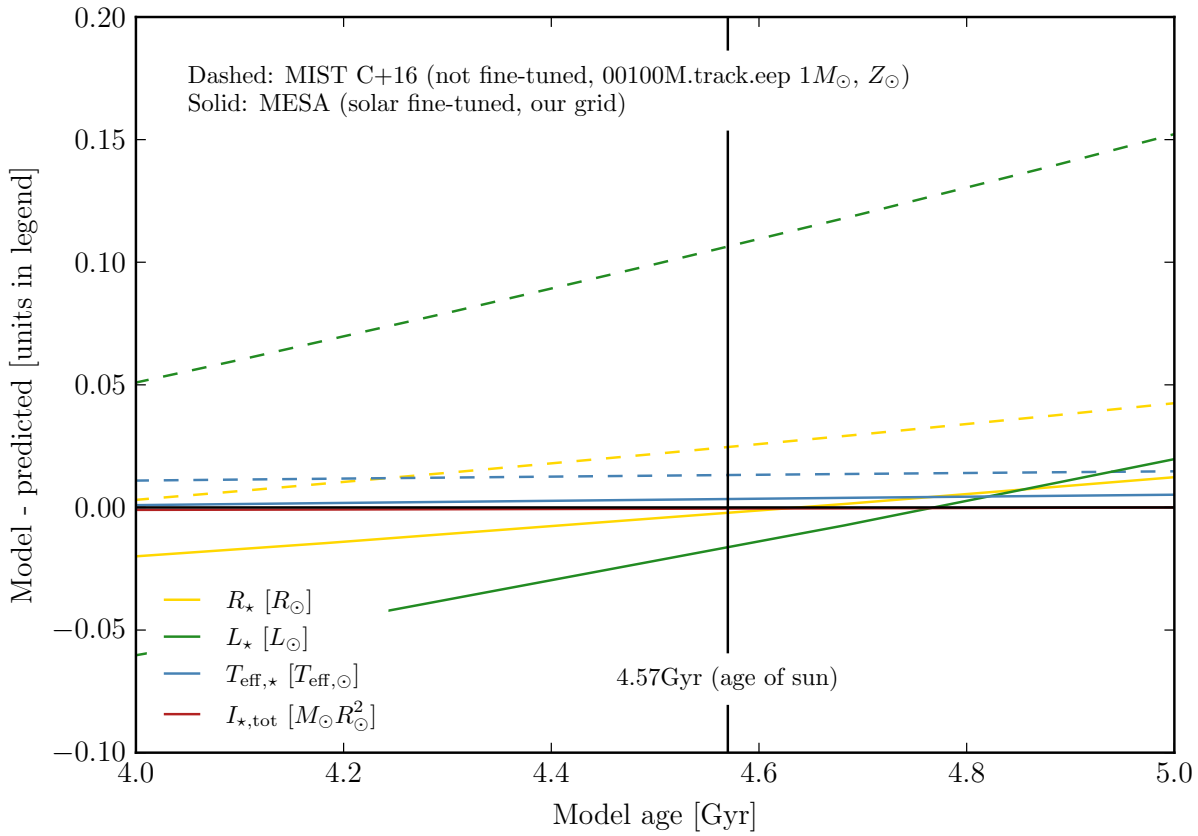

Figure 2: Solar calibration (see Sec. 1.2 for description).

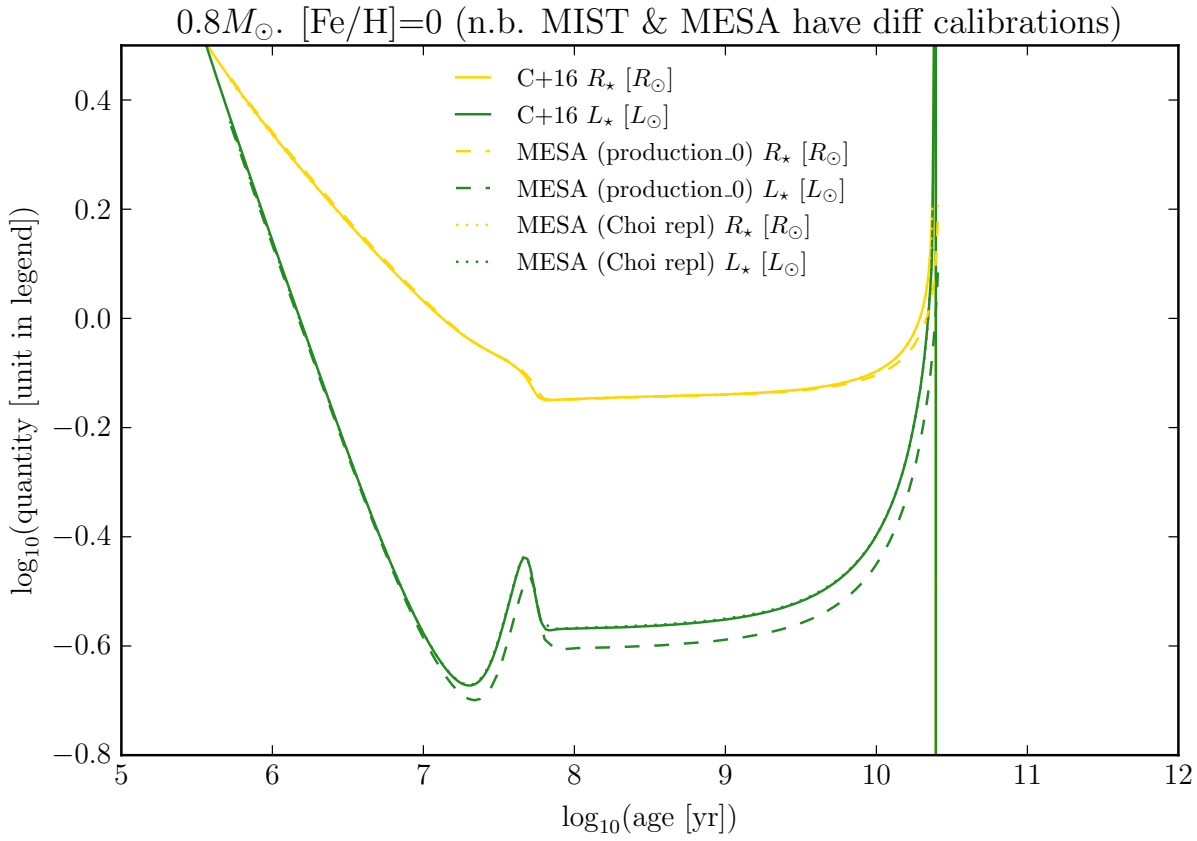

Figure 3: Replicating the MIST models (close enough that I'm OK calling them 'replicated') in the `Choi_repl` MESA grids. This plot is for $M_\star = 0.8M_\odot$, [Fe/H] = 0 ($Z = 0.015$ for the `production_0` grids, $Z = 0.0142$ for `Choi_repl`.

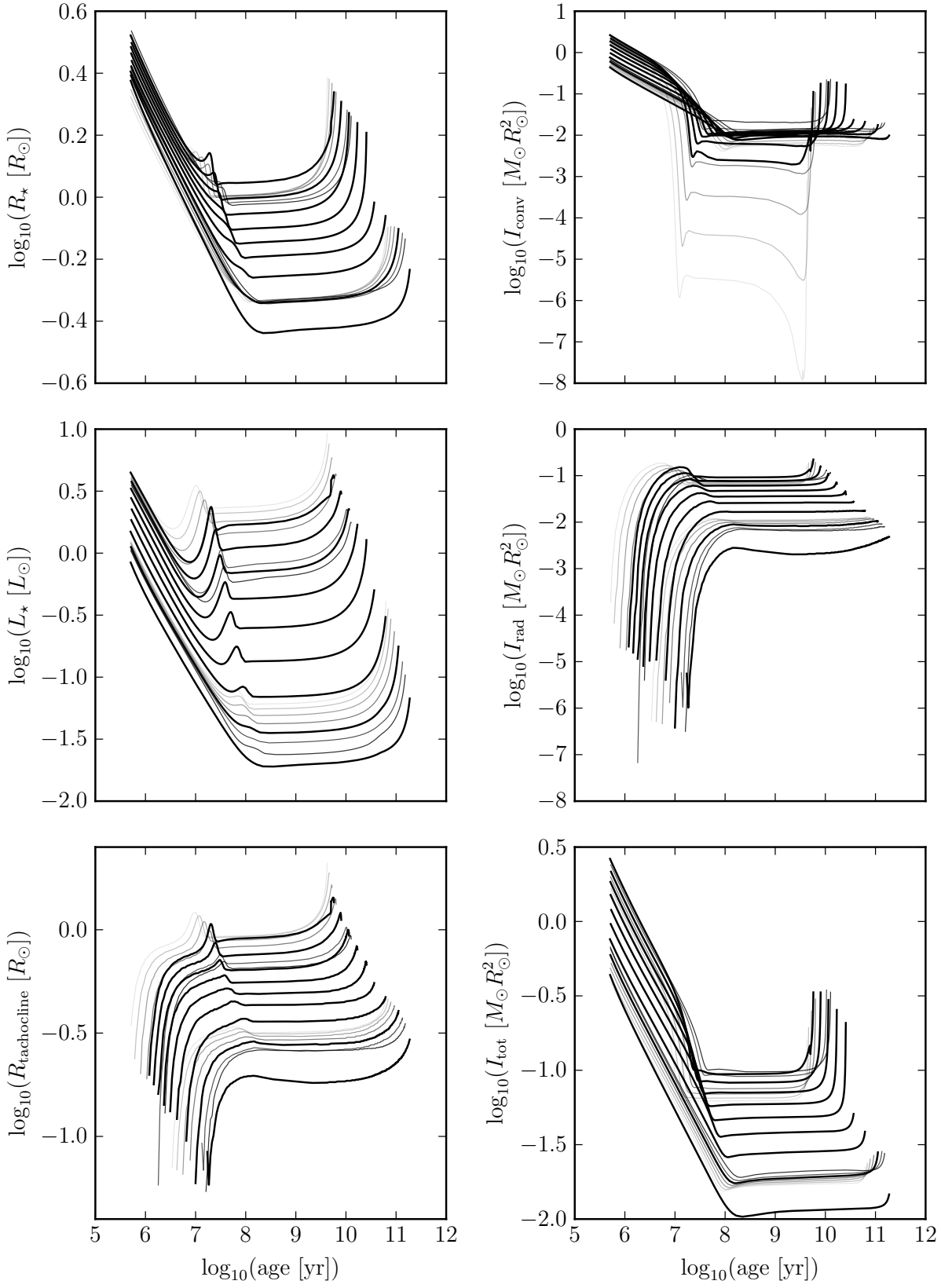

Figure 4: Stellar evolutionary grids from $0.4 - 1.2 M_\odot$ (more massive means bigger radius and ∼smaller convective moment of inertia during MS lifetime). The thick black lines are [Fe/H] = 0 ($Z \equiv Z_\odot = 0.015$) models, varying over mass. The thinner gray lines vary [Fe/H] = −1 to 0.5, where fainter means lower metallicity. They are shown for 1.1 and $0.5 M_\odot$.